

Elastic and inelastic scattering of 12.0-MeV protons from $^{84,86}\text{Kr}^\dagger$

B. K. Arora, D. K. Olsen,* P. J. Riley, and C. P. Browne ‡

Center for Nuclear Studies, The University of Texas, Austin, Texas 78712

(Received 24 June 1974)

Differential cross sections for elastic and inelastic scattering of 12.0-MeV protons from ^{84}Kr and ^{86}Kr have been measured. Optical-model parameters obtained from the elastic cross sections were used in distorted-wave-Born-approximation and coupled-channel calculations in order to determine the spin, parities, and deformation parameters of excited states. The deformation parameters found are $\beta_2 = 0.128$ and 0.108 for the first 2^+ states in ^{84}Kr and ^{86}Kr , respectively, and are $\beta_3 = 0.158$ and 0.145 , respectively, for the first 3^- states. Most of the scattering strength to the "two-phonon" states proceed through their one-phonon components. The spins of several higher excited states are suggested.

[NUCLEAR REACTIONS $^{84,86}\text{Kr}(p, p')$, $E = 12.0$ MeV; measured $\sigma(\theta)$ and level energies; deduced optical-model parameters, J^π and β from DWBA and coupled channels.]

I. INTRODUCTION

The interpretation of inelastic scattering as a direct nuclear reaction with phenomenological nuclear models provides spectroscopic information on the properties of low-lying collective states in even-even nuclei. In particular, the macroscopic vibrational model of Bohr¹ provides a basis for understanding these states in spherical nuclei in terms of phonon vibrations with time-averaged mass deformation parameters β . Using this model, the lowest-energy 2^+ and 3^- states in spherical nuclei have been extensively investigated with inelastic scattering, and have been interpreted as one-quadrupole and one-octupole phonon vibrations which are excited by a single-step process described with the distorted-wave-Born-approximation (DWBA) formalism. If the cross sections to these one-phonon states are large, the more sophisticated coupled-channel formalism,^{2,3} in which the interactions are considered to infinite order, gives a better reproduction of the experimental data. On the other hand, pure two-phonon vibrational states are also very collective, but cannot be populated by a single-step process and hence must be described by the coupled-channel formalism. It has been established, however, that many two-phonon states are not pure, at least in the Cd region, and that much of their inelastic scattering strength comes from their one-phonon admixtures.⁴

In this paper we report the measurement of differential cross sections for elastic and inelastic scattering of 12.0-MeV protons from 22 states in ^{84}Kr and ^{86}Kr . These experimental results are compared with DWBA calculations in order to deduce the spins and parities of the residual levels

I^π and their mass deformation parameters β_γ .

In addition, coupled-channel calculations have been performed for many levels of ^{84}Kr and ^{86}Kr in order to investigate the extent to which these states can be described as two-phonon vibrations.

The level structure of both ^{84}Kr and ^{86}Kr has been previously studied. Spins and parities were assigned on the basis of γ -ray intensities and $\log ft$ values in the radioactive β decay of $^{84}\text{Br}^{5-7}$ and $^{86}\text{Br}^{8-10}$; however, these assignments were not unique except for a very few low-lying states. The deuteron inelastic scattering on ^{86}Kr by Rosner and Schneid,¹¹ the $^{87}\text{Rb}(t, \alpha)$ work by Tucker *et al.*,¹² and the $^{84}\text{Kr}(t, p)$ work by Riley *et al.*,¹³ yielded information on ^{86}Kr . Neutron capture¹⁴ measurements for ^{84}Kr primarily determined excited-state energies, whereas Heydenburg, Pieber, and Anderson¹⁵ measured relative $B(E2)$ values for the first 2^+ state of several even-even krypton isotopes. In addition, McCauley and Draper¹⁶ have investigated ground-state quasi-rotational bands in the even krypton isotopes. Some inelastic proton scattering has been done on ^{86}Kr ; however, the primary emphasis was on ^{87}Rb isobaric analog levels.¹⁷ In spite of all this work comparatively little is known about the level structure of ^{84}Kr and ^{86}Kr .

In the present work concrete spin assignments for excited levels are also difficult to make; however, several definite and many tentative assignments are possible. In particular, we confirm the previously tentative⁵ 0^+ assignment for the 1837-keV level in ^{84}Kr . We find that neither ^{84}Kr , which is two neutrons below the 50-neutron shell closure, nor ^{86}Kr which is at the 50-neutron shell closure, is described well by a vibrational model, and that nearly all of the inelastic strength to the

“two-phonon” states proceed through their one-phonon components.

II. EXPERIMENTAL APPARATUS

A 12.0-MeV proton beam from the University of Texas at Austin EN tandem Van de Graaff accelerator was focussed through a 3.2-mm collimator onto target gas contained in a 7.62-cm-diam thin walled gas cell. After passing through the target, the beam was collected in a 25.4-cm-diam 305-cm-long Faraday cup and measured with a BIC Model 1000C current integrator. The walls of the gas cell were made of 3.0- μ m Mylar foils with 0.79-cm by 1.11-cm beam entrance and exit windows. These beam windows were covered with 0.63- μ m nickel foils.

The resultant elastic and inelastic protons from the target gas were simultaneously detected in four different detector assemblies spaced at 20° intervals on a rotatable plate on the bottom of a 50.8-cm-diam scattering chamber. Each detector assembly defined a gas target geometry factor G using the usual two slit arrangement.¹⁸ A typical value of G was 5.2×10^{-4} cm. The charged particle reaction products were counted with 2.0-mm-thick, lithium-drifted silicon solid-state detectors cooled to dry-ice temperatures. Measurements were made with 99.9% isotopically pure ⁸⁶Kr, 90.1% isotopically pure ⁸⁴Kr, and natural krypton gas which contains 17.4% ⁸⁶Kr, 56.9%

⁸⁴Kr, 11.6% ⁸³Kr, 11.6% ⁸²Kr, 2.3% ⁸⁰Kr, and 0.4% ⁷⁸Kr. The pressure of the gas in the cell was measured within 2% error with a Wallace and Tierman Model 15304 gauge which was calibrated with a precision oil manometer. An overall energy resolution (full width at half-maximum) of roughly 35 keV was obtained with a gas pressure of 0.025 atm. Data were taken with about 200 nA of beam current with typical collection of 1800 to 5200 μ C of charge.

III. EXPERIMENTAL PROCEDURES AND RESULTS

Spectra were obtained in 5° intervals from 30° to 160° with both the isotopically enriched ⁸⁴Kr and ⁸⁶Kr targets. Four spectra were measured simultaneously, and many angles were repeated several times, both with the same detector assembly and with different detector assemblies, in order to insure consistency in the data. The bottom part of Fig. 1 shows a typical spectrum from the ⁸⁴Kr gas at 80°. This is compared with the spectrum shown in the top part of Fig. 1 obtained from natural krypton gas at the same angle, in order to facilitate identification of the proton groups from other krypton isotopes. Elastic proton groups from oxygen and nitrogen contaminations were observed at all angles. No ⁸³Kr states and only the one-phonon 2⁺ and 3⁻ states of ⁸⁶Kr were observed on the ⁸⁴Kr spectra. Figure 2 shows a similar spectrum from ⁸⁶Kr gas at

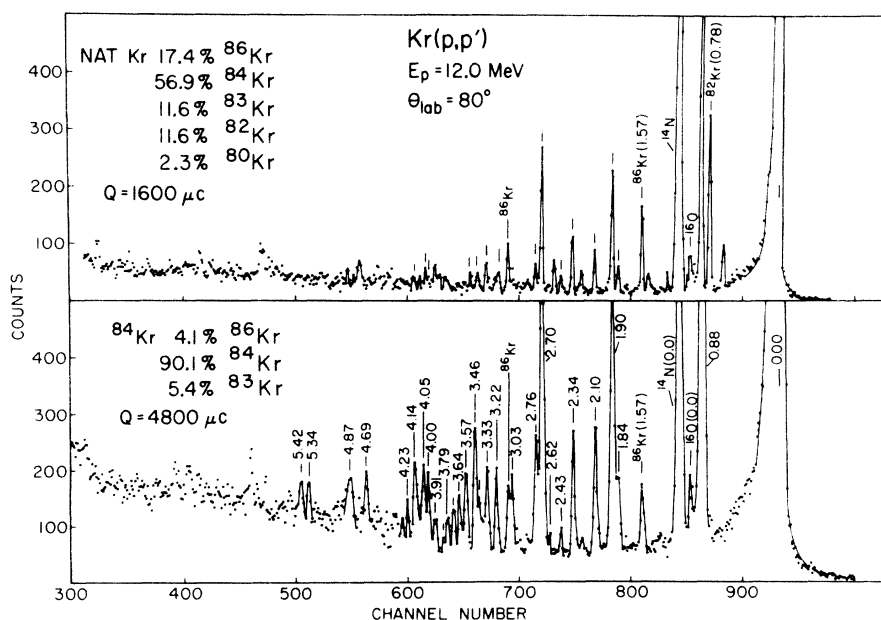


FIG. 1. Sample ⁸⁴Kr(p, p')⁸⁴Kr spectrum (bottom) taken with 12.0-MeV protons at 80°. This spectrum is compared with a natural krypton spectrum (top) taken at the same proton energy and angle in order to facilitate the identification of proton groups from other isotopes. The isotopic abundances of the target gases are given in the figure. The excitation energies of all the ⁸⁴Kr proton groups are listed in Table I.

120°. Because the ^{86}Kr gas was 99.9% isotopically pure, only oxygen and nitrogen contaminant peaks were observed.

The Q values for inelastic scattering to 25 states in ^{84}Kr and 32 states in ^{86}Kr were measured. Particle energies were found by performing a linear, least-squares fit on the laboratory energies of the measured elastic and inelastic proton groups. In addition to the elastic groups, calibration energies were obtained using the low-lying excitation energies determined from Li(Ge)-detector γ -ray work.^{5,10} Each set of excitation energies shown in Tables I and II is the average of those taken from six spectra. Corrections for the energy loss suffered by protons while passing through the target gas, Mylar walls and nickel window were made using the tables of Williamson and Boujot.¹⁹ The over-all error in the excitation energies is estimated to be less than 10 keV for the low-lying states and somewhat larger for the higher excited states because the laboratory energy scale was extrapolated downwards. As shown in Table I and II our excitation energies are in reasonable agreement with those measured by other workers; however, we observe many new states. The state observed at 3080 keV in ^{84}Kr by other workers perhaps is in fact the ^{86}Kr one-phonon 3^- state at $E_x = 3.096$ MeV.

The measured differential cross sections for elastic and inelastic scattering are shown in Figs. 3 to 11. Where the data point is not accompanied with an error bar the relative error of that point due to counting statistics is less than 3%. The uncertainty in the absolute cross section scale is estimated to be 5%. These differential cross sections and the curves shown on the figures will be discussed in detail in the next section.

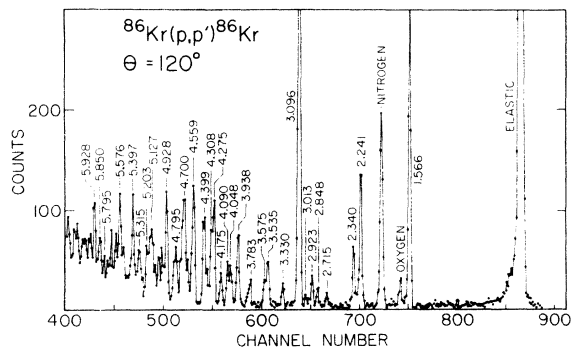


FIG. 2. Sample $^{86}\text{Kr}(p, p')^{86}\text{Kr}$ spectrum taken with 12.0-MeV protons at 120°. The target gas was 99.9% isotopically pure. Most of the weaker proton groups could only be clearly observed at backward angles. The ^{86}Kr excitation energies are listed in Table II.

IV. ANALYSIS

A. Optical-model parameters

The differential cross sections for elastic scattering from both ^{84}Kr and ^{86}Kr are shown in Fig. 3 (plotted as the ratio-to-Rutherford) where the smooth curves are best optical-model fits to these data. These fits were obtained using the computer code of Smith²⁰ starting with the average optical-model parameters of Perey.²¹ Keeping Perey's average real, imaginary, and Coulomb radii parameters ($r_R = r_I = r_C = 1.25$ fm) fixed and also his average spin-orbit parameters ($r_{so} = 1.25$ fm, $a_{so} = 0.65$ fm, $V_{so} = 7.5$ MeV) fixed, both the real and imaginary diffusenesses (a_R and a_I) and real and surface imaginary well depths (V_R and W_D) were allowed to vary in order to minimize the usual χ^2 quantity. The final set of optical-potential parameters for both ^{84}Kr and ^{86}Kr are listed in Table III, where the χ^2 per point for these best

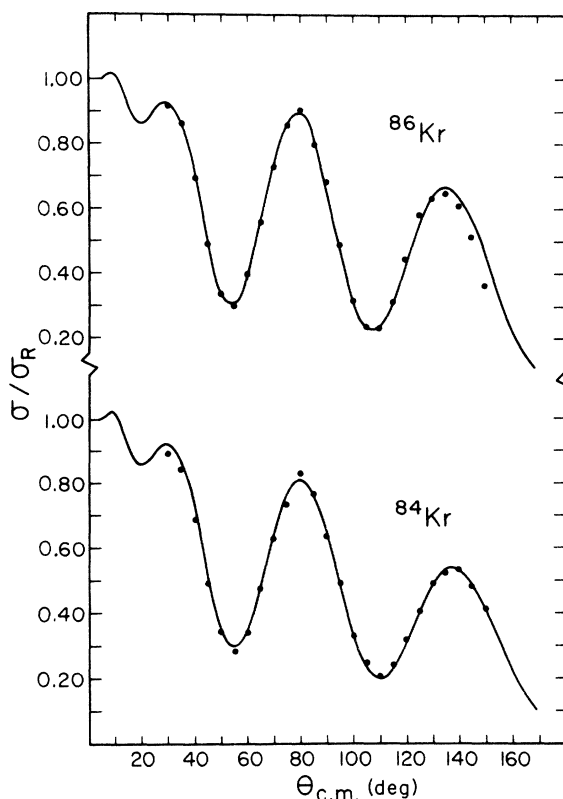


FIG. 3. Comparison of optical-model fits to the experimental ratio-to-Rutherford cross sections for elastic scattering of 12.0-MeV protons from ^{86}Kr and ^{84}Kr . The optical-model parameters are given in Table III. The solid line also represents the coupled-channel prediction for the elastic cross sections, because reducing the surface imaginary depth by 5 to 15%, depending on the coupling scheme used, restored the coupled-channel elastic cross section to within a very few percent of the optical-model fit.

TABLE I. Excitation energies E_x and spins and parities of ^{84}Kr levels. The over-all errors of the E_x from the present work are estimated to be less than 10 keV for the low-lying states and 20 keV for the higher excited states.

Present work		Hill and Wang (Ref. 5)		Hattula <i>et al.</i> (Ref. 7)		Mattsson <i>et al.</i> (Ref. 14)	
E_x (MeV)	I^π	E_x (MeV)	I^π	E_x (MeV)	I^π	E_x (MeV)	I^π
0.00	0 ⁺	0.00	0 ⁺	0.00	0 ⁺	0.00	
0.882	2 ⁺	0.882	2 ⁺	0.882	(2) ⁺	0.882	
1.834	0 ⁺	1.837	(0 ⁺)				
1.900	2 ⁺	1.898	2 ⁺	1.898	(2) ⁺	1.898	
2.086	4 ⁺	2.094	4 ⁺	2.095	(4) ⁺	2.095	
2.337	4 ⁺	2.345		2.344	(4) ⁺	2.345	
...		2.489					
2.626		2.623	(1, 2)	2.622	(2, 3) ⁺	2.624	
2.705	3 ⁻	2.700	2, 3	2.700	(3) ⁻	2.700	
...		2.759	1, 2	2.759	(1, 2) ⁺	2.761	
2.775	2 ⁺			2.768	(5) ⁻	2.770	
3.048						3.040	(3, 4, 5, 6)
...		3.082	2, 3	3.082	(2, 3) ⁺	3.082	
3.225	(1 ⁻)					3.218	(3, 4, 5, 6)
...		3.366	1, 2	3.366	(1, 2) ⁺		
3.335							
3.477	1 ⁻	3.475	1, 2, 3	3.476	(4) ⁺		
3.570	3 ⁻					3.587	(3, 4, 5, 6) ⁻
3.650	5 ⁻					3.638	(3, 4, 5, 6) ⁻
3.721	(3 ⁻)	3.706	1, 2, 3	3.706	(2, 3) ⁺	3.715	(3, 4, 5, 6) ⁻
3.795							
...		3.870	1, 2, 3				
...		3.879	1, 2, 3				
3.916		3.927	1 ⁻	3.928	(1, 2) ⁻		
4.006						4.000	(3, 4, 5, 6) ⁻
...		4.084	(1 ⁺ , 2 ⁺)				
4.061				4.084	(1, 2) ⁺		
...		4.116	1 ⁻ , 2 ⁻ , 3 ⁻	4.117	(2, 3) ⁻		
4.157							
...		4.189	1, 2, 3				
4.707							
4.898							
5.358							
5.466							

fits were about one with 3% error bars for the experimental data. In addition, this procedure was repeated with different normalizations of the experimental elastic cross sections to insure that the χ^2 was a true minimum with respect to the measured absolute cross section scale. These optical-model parameters were used in the following distorted-wave Born-approximation (DWBA) and coupled-channel analyses.

B. DWBA analysis

A DWBA analysis was performed on the differential cross sections to twelve excited states of ^{84}Kr and eight excited states of ^{86}Kr with the computer code JUPITOR-1²² in order to determine the deformation parameters β_I and spins and par-

ities I^π of these states. Many of these states were also investigated with coupled-channel calculations; in which case, the DWBA results provided a starting point for the more involved coupled-channel analysis. JUPITOR-1 was used to obtain DWBA cross sections by performing calculations with a one-phonon coupling scheme taking $\beta_I = 0.01$. With this small deformation parameter, the effect of the coupling is negligible. The DWBA deformation parameters were then determined by scaling the calculated cross sections by β_I^2 to give the best visual fits to the experimental cross sections. The exact optical-model parameters of the previous section were used with both real and imaginary form factors. The amplitudes from Coulomb excitation were not considered because of the large computer time needed to include this effect.

TABLE II. Excitation energies E_x and spins and parities of ^{86}Kr levels. The over-all errors of the E_x from the present work are estimated to be less than 10 keV for the low-lying states and 20 keV for the higher excited states.

Present work		Riley <i>et al.</i> (Ref. 13)		Tucker <i>et al.</i> (Ref. 12)		Achterberg <i>et al.</i> (Ref. 10)	
E_x (MeV)	I^π	E_x (MeV)	I^π	E_x (MeV)	I^π	E_x (MeV)	I^π
0.00	0 ⁺	0.00	0 ⁺	0.00	0 ⁺	0.00	0 ⁺
1.566	2 ⁺	1.565	2 ⁺	1.565	2 ⁺	1.565	2 ⁺
2.241	4 ⁺	2.248	4 ⁺	2.249	4 ⁺		
2.340	2 ⁺	2.355	2 ⁺	2.346	2 ⁺	2.350	(1, 2)
2.715		2.733	0 ⁺	2.724	(0 ⁺)		
2.848				2.847	(2 ⁺)	2.850	
2.923				2.917	(3, 4)	2.926	(1, 2)
3.012				3.010	(1, 2) ⁺	3.009	
3.096	3 ⁻	3.109	3 ⁻			3.099	(3 ⁻)
3.330	(4 ⁺)			3.322	0 ⁺ , 1 ⁺ , 2 ⁺		
3.535		3.542	0 ⁺	3.534	0 ⁺ , 1 ⁺ , 2 ⁺		
3.575							
3.783				3.783	1 ⁺ , 2 ⁺	3.782	
3.809		3.832	0 ⁺				
3.938	(5 ⁻)	3.959	(3 ⁻ , 4 ⁺ , 5 ⁻)	3.930			
4.048		4.072		4.037	(3 ⁻)	4.038	
4.090		4.111	2 ⁺				
4.175	(4 ⁺)	4.194	2 ⁺	4.173		4.164	
4.275		4.298	(2 ⁺)	4.277			
4.308						4.316	(2 ⁻ , 3 ⁻)
4.399							
4.559							
...		4.668	(2 ⁺)				
4.700		4.708	(4 ⁺)				
4.795		4.826	2 ⁺				
4.928	(4 ⁺)	4.948	(2 ⁺)				
...		4.991					
5.127							
5.203							
5.315							
5.397							
5.576							
5.795							
5.850							
5.928							

Figure 4 shows the DWBA fits to the cross sections of the one-quadrupole phonon states 2_1^+ at 0.882-MeV and 1.566-MeV of excitation in ^{84}Kr and ^{86}Kr , respectively. The calculations fit the shapes of the experimental angular distributions well, particularly ^{84}Kr . The strength of these transitions are given by $\beta_2 = 0.131$ and 0.106, respectively, for ^{84}Kr and ^{86}Kr . Similarly Fig. 5 shows the DWBA fits to the one-octupole phonon states 3_1^- . Again the experimental shapes of the

angular distributions are reproduced reasonably well, with that of ^{84}Kr being best. The strengths of these transitions are given by $\beta_3 = 0.157$ and 0.142, respectively, for ^{84}Kr and ^{86}Kr . The deformation parameters for these states are summarized in Table IV.

The DWBA deformation parameters for the "two-phonon" states were also determined. With the pure vibrational model¹ these states, of course, cannot be excited with a single-step (DWBA) pro-

TABLE III. Optical-model parameters for 12.0-MeV protons.

Target	r_R	a_R	V_R	r_I	a_I	W_D	r_{so}	a_{so}	V_{so}	r_c
^{84}Kr	1.25	0.646	53.2	1.25	0.467	14.9	1.25	0.65	7.5	1.25
^{86}Kr	1.25	0.604	53.5	1.25	0.565	10.6	1.25	0.65	7.5	1.25

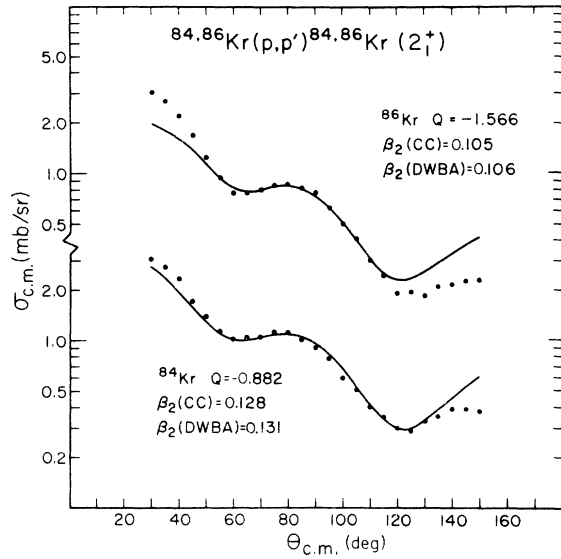


FIG. 4. Measured differential cross sections for exciting the one-quadrupole phonon states in ^{84}Kr and ^{86}Kr with 12.0-MeV protons. The best visual fits to the experimental data for both coupled-channel and DWBA calculations are shown by the smooth curves with the corresponding deformation parameters given in the figure. The difference between the coupled-channel and DWBA predicted cross sections is negligible.

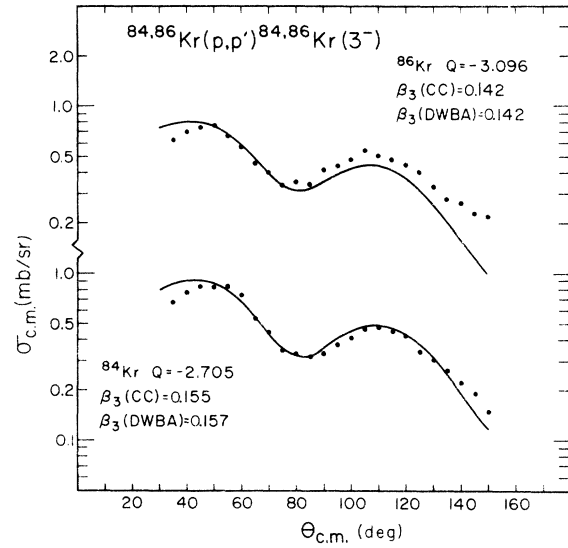


FIG. 5. Measured differential cross sections for exciting the one-octupole phonon states in ^{84}Kr and ^{86}Kr with 12.0-MeV protons. The best visual fits to the experimental data for both coupled-channel and DWBA calculations are shown by the smooth curves with the corresponding deformation parameters given in the figure. The difference between the coupled-channel and DWBA predicted cross sections is negligible.

cess; however, it is well known that much of the strength to these states comes from their wave function's one-phonon admixtures. The dashed curves in Figs. 6 and 7 show the DWBA fits to the cross sections of the likely "two-phonon" states in ^{84}Kr . In particular these are the first excited 0^+ state at 1.834 MeV, the second 2^+ state at 1.900 MeV and two 4^+ states at 2.086 and 2.337 MeV. In all cases, the shapes of the angular distributions are not fitted well by the DWBA. The deformation parameters from these DWBA fits are given in the last column of Table V.

Only two states in ^{86}Kr have the correct excita-

TABLE IV. Deformation parameters for one-phonon quadrupole and octupole vibrations determined from DWBA and coupled-channel calculations.

Target	Coupling scheme	β_2	β_3
^{84}Kr	DWBA	0.131	0.157
	$0_1^+ - 2_1^+$ and $0_1^- - 3_1^-$	0.128	0.160
	$0_1^+ - 2_1^+ - 3_1^-$	0.128	0.155
^{86}Kr	DWBA	0.106	0.142
	$0_1^+ - 2_1^+$ and $0_1^- - 3_1^-$	0.108	0.145
	$0_1^+ - 2_1^+ - 3_1^-$	0.105	0.142

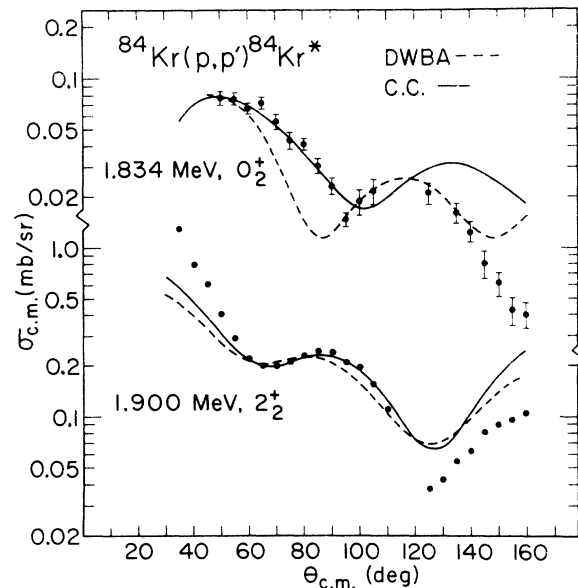


FIG. 6. Measured differential cross sections for exciting the 0_2^+ and 2_2^+ states in ^{84}Kr with 12.0-MeV protons. The dashed curves are DWBA fits with $\beta_0 = 0.019$ and $\beta_2 = 0.063$. The solid curves are coupled-channel fits assuming these states to be two-quadrupole phonon vibrations with large one-phonon admixtures. The deformation parameters are summarized in Table V.

TABLE V. Coupled-channel β_{0I}^* and DWBA β_I deformation parameters for two-quadrupole phonon states. For the coupled-channel calculations $\beta_{02} = \beta_{2I} = \beta_{0I}^* = 0.128$ and 0.105 for ^{84}Kr and ^{86}Kr , respectively. DWBA analysis does not determine the sign of β_I .

Target	I^π	Energy (MeV)	β_{0I}^*	β_I
^{84}Kr	2_2^+	1.900	0.062	0.063
	0_2^+	1.834	-0.012	0.019
	4_1^+	2.086	0.057	0.064
	4_2^+	2.337	0.048	0.056
^{86}Kr	2_2^+	2.340	0.045	0.047
	4_1^+	2.241	0.069	0.079

tion energy to be considered possible "two-phonon" excitations; a 4^+ state at 2.241 MeV and a 2^+ state at 2.340 MeV. The DWBA fits to these cross sections are shown in Fig. 8 and the extracted deformation parameters are also given in Table V. In particular, note the poor fit to the angular distribution to the second 2^+ state which is considerably different from the corresponding state in ^{84}Kr and the one-phonon states in both ^{84}Kr and ^{86}Kr .

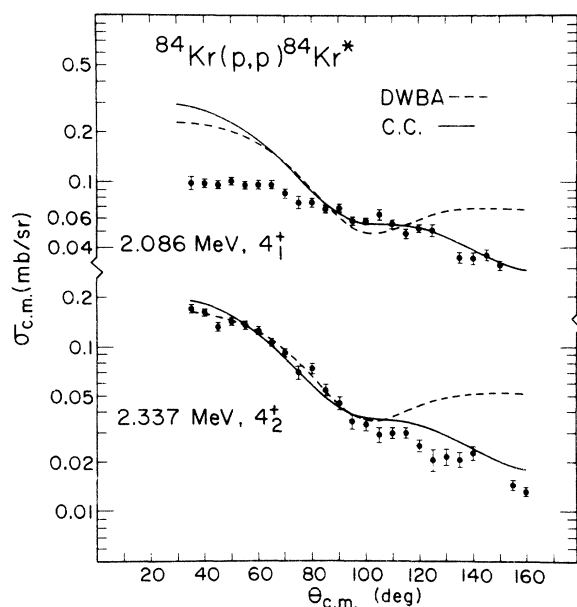


FIG. 7. Measured differential cross sections for exciting the 4_1^+ and 4_2^+ states in ^{84}Kr with 12.0-MeV protons. The dashed curves are DWBA fits with $\beta_4 = 0.064$ and 0.056, respectively. The solid curves are coupled-channel fits assuming these states to be two-quadrupole phonon vibrations with large one-phonon admixtures. The deformation parameters are summarized in Table V.

Most of the other proton groups recorded on the ^{84}Kr and ^{86}Kr spectra had widths which indicated that they were doublets, or rose above the background sufficiently for a quantitative analysis only at very backward angles. However, 10 other strong groups appeared to arise from single transition. In particular cross sections to three states in ^{84}Kr at 3.477, 3.570, and 3.650 MeV of excitation were measured and are shown in Fig. 9. The smooth curves are the best DWBA fits to these data and were obtained for $I^\pi = 1^-, 3^-,$ and 5^- , respectively, with deformation parameters of $\beta_1 = 0.057$, $\beta_3 = 0.063$, and $\beta_5 = 0.051$. These states have excitation energies very near to the sum of the energies of the one-phonon quadrupole and octupole states and perhaps contain a large admixture of two-phonon quadrupole-octupole vibration.

Figure 10 shows cross sections to three isolated states in ^{84}Kr at 2.775, 3.225, and 3.721 MeV of excitation where the DWBA smooth curves indicate that these states perhaps have $I^\pi = 2^+, 1^-,$ and 3^- , respectively, with deformation parameters very close to 0.04. The fit to the 2^+ state is very good, whereas the fit to the 1^- state is perhaps speculative. Only four higher excited states in ^{86}Kr appeared to be sufficiently isolated to allow cross-

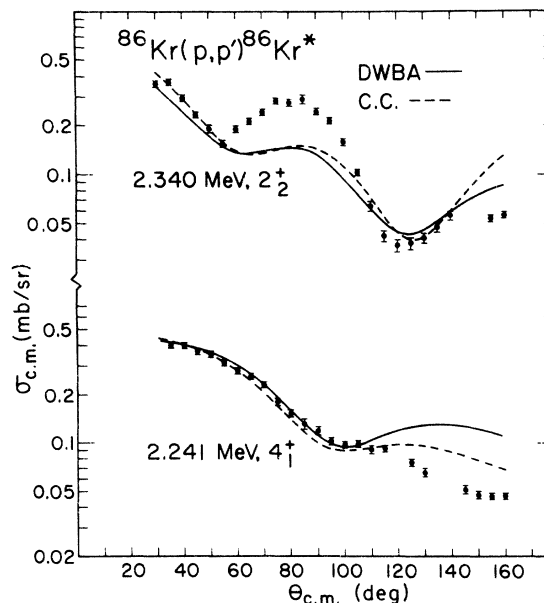


FIG. 8. Measured differential cross sections for exciting the 2_2^+ and 4_1^+ states in ^{86}Kr with 12.0-MeV protons. The solid curves are DWBA fits with $\beta_2 = 0.047$ $\beta_4 = 0.079$. The dashed curves are coupled-channel fits assuming these states to be two-quadrupole phonon vibrations with large one-phonon admixtures. The deformation parameters are summarized in Table V. Note the shape of this 2^+ angular distribution with those on Figs. 4 and 6.

section measurements. These are shown in Figure 11. Three of these states at 3.330, 4.175, and 4.928 MeV could perhaps be 4^+ states with $\beta_4 = 0.031$, 0.042, and 0.098, respectively, whereas the state at 3.939 MeV of excitation is best fit as a $1^\pi = 5^-$ with $\beta_5 = 0.10$. Many of these experimental cross sections were also compared with coupled-channel calculations.

C. Coupled-channel analysis

Using the optical-model potentials and mass deformations determined in the previous two subsections as starting parameters, coupled-channel calculations were performed for the cross sections to the one-phonon quadrupole and octupole states in ^{84}Kr and ^{86}Kr , possible two-quadrupole phonon states in ^{84}Kr and ^{86}Kr , and possible octupole-quadrupole phonon states in ^{84}Kr . With the coupled-channel formalism, the inelastically scattered waves are obtained from potentials which undergo vibrations about a spherical shape. The coupling potentials are expanded to second order in the deformation parameters and the solution with these potentials is carried out to infinite order. Extensive details of the formalism are given in Ref. 2. Usually, for vibrational nuclei, the exact

optical potential determined from a standard optical-model analysis are used except for the surface imaginary well depth W_D . Part of the absorption is now explicitly taken into account by the coupling potentials and hence the absorption implicit in W_D must be reduced. As with the previous DWBA analysis, complex form factors were used and Coulomb excitation was not considered.

1. One-phonon quadrupole and octupole states

Cross sections to the ^{84}Kr and ^{86}Kr one-quadrupole and one-octupole phonon states were fitted using two different coupling schemes. The first method considered $0_1^+ - 2_1^+$ and $0_1^+ - 3_1^-$ couplings separately, whereas the second method used $0_1^+ - 2_1^+ - 3_1^-$ coupling schemes. Explicitly coupling in the inelastic channels reduces the elastic cross section. For vibrational nuclei, the ground state remains spherical and slightly reducing W_D restores the optical fit to the elastic cross sections almost exactly. The correct optical parameters for the excited states are, of course, unknown and those determined from the elastic fits were used. With the $0_1^+ - 2_1^+$ couplings the optical fits were restored by reducing W_D by 10 and 5% for ^{84}Kr and ^{86}Kr , respectively, and the $0_1^+ - 3_1^-$ couplings

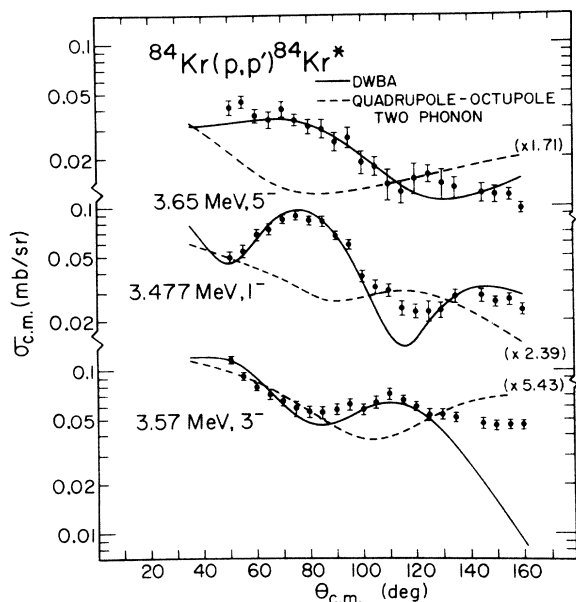


FIG. 9. Measured differential cross sections for exciting states at 3.650, 3.477, and 3.570 MeV of excitation in ^{84}Kr with 12.0-MeV protons. The solid curves are DWBA fits assuming these states to be 5^- , 1^- , and 3^- , respectively, with $\beta_5 = 0.051$, $\beta_1 = 0.057$, and $\beta_3 = 0.051$. The dashed curves, divided by the numbers in parentheses, are coupled-channel predictions assuming these states to be octupole-quadrupole vibrations with $\beta_3 = 0.155$ and $\beta_2 = 0.128$.

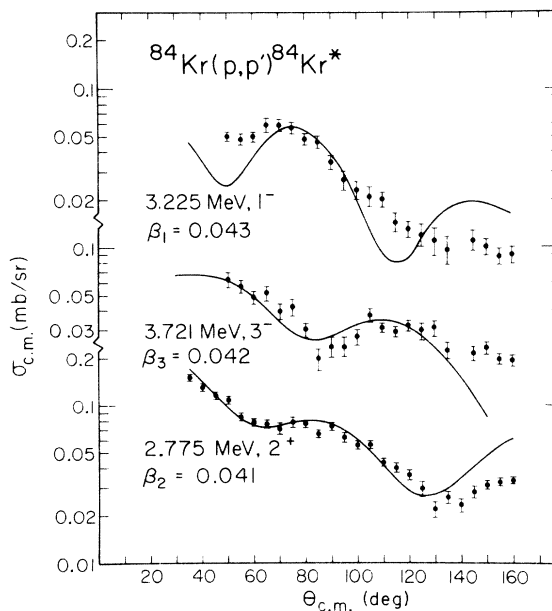


FIG. 10. Measured differential cross sections for exciting states in ^{84}Kr at 3.225, 3.721, and 2.775 MeV of excitation with 12.0-MeV protons. The smooth curves are DWBA, best-visual fits to these cross sections assuming the states to be 1^- , 3^- , and 2^+ , respectively. The fit to the 2.775-MeV angular distribution is very good, whereas the fit to the 3.225-MeV angular distribution is perhaps speculative. The deformation parameters are given in the figure.

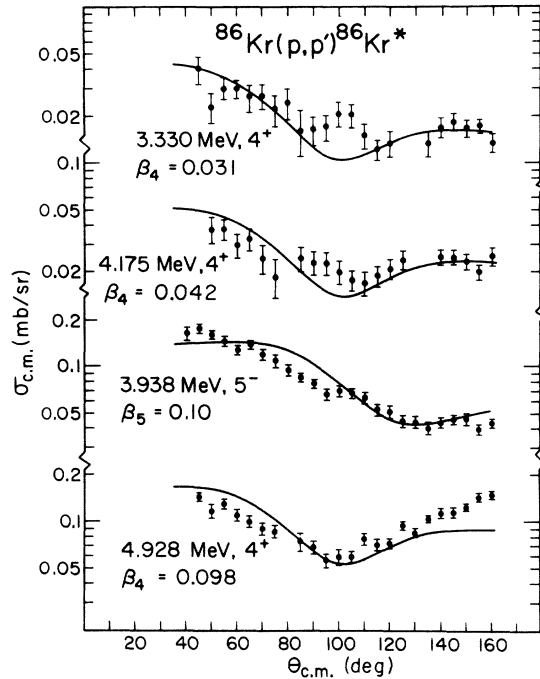


FIG. 11. Measured differential cross sections for exciting states in ^{86}Kr at 3.330, 4.175, 3.938, and 4.918 MeV of excitation with 12.0-MeV protons. The cross sections to these states are relatively flat and are fitted best with high angular momentum transfers as shown.

required W_D to be reduced by 5% for both isotopes. With both the 2_1^+ and the 3_1^- states coupled to the elastic channel the imaginary strengths were reduced further; 13% for ^{84}Kr and 10% for ^{86}Kr . The deformation parameters required to fit the one-phonon strengths are summarized in Table IV and are nearly the same for the DWBA and both coupled-channel coupling schemes. Furthermore, the fit to the elastic, 2_1^+ and 3_1^- cross sections are the same within a few percent for DWBA and coupled channels, so each smooth curve shown in Figs. 3–5 is the result of three different calculations.

2. Two-quadrupole phonon states

Coupled-channel calculations were performed for strongly excited states at roughly twice the excitation energies of the one-quadrupole phonon states, which could be considered candidates for two-quadrupole phonon states. In ^{84}Kr there are four such states; a 0_2^+ state at 1.83 MeV of excitation, a 2_2^- state at 1.90 MeV, and two 4^+ states at 2.10 and 2.34 MeV. In ^{86}Kr there is only a 4_1^+ state at 2.241 MeV and a 2_2^+ state at 2.340 MeV.

The many mass deformation parameters β needed to describe the excitation of these states

are defined in complete detail in Ref. 2 and are only briefly discussed here. In addition to the usual β_{02} to the one-phonon 2^+ state, there is a β_{2I} which connects the one-phonon 2^+ to the two-quadrupole phonon state of spin I where $I = 0, 2$, or 4. The deformation parameter β'_{0I} connecting the ground state to the two-phonon state, arises from the second order expansion of the potentials, and is usually set equal to $(\beta_{02}\beta_{2I})^{1/2}$. If the two phonon state is pure, then $\beta_{02} = \beta_{2I} = \beta'_{0I}$; however, experimentally this is usually not the case, and a deformation parameter β''_{0I} is introduced which is a measure of the one-phonon admixture in the two-phonon state and is analogous to the β_I parameter from the DWBA analysis. Both the magnitude and sign of β''_{0I} affect the cross section because there is interference between the direct path and two-step path through the 2_1^+ state.

The angular distributions to these states are fitted very poorly when treated as pure two-phonon vibrations; the cross sections have the wrong shape and are considerably smaller than the experimental data. The fits to these states are markedly improved when a one-phonon component ($\beta''_{0I} \neq 0$) is allowed in their wave functions. In fact most of the strength to these states comes from their one-phonon components.

With both one- and two-phonon components, the previously determined β_{02} were kept fixed. The β_{2I} were incremented from 0.0 to $+\beta_{02}$ with both the magnitudes and signs of the β'_{0I} varied for each value of β_{2I} to give the best visual fit to the experimental cross sections. The β'_{0I} were always set equal to $(\beta_{02}\beta_{2I})^{1/2}$. Using this procedure it was found that the cross sections were somewhat insensitive to the two-step path and that the best fit to the data were with $\beta_{0I} = \beta_{02}$ for all the states. Allowing the $\beta_{0I} > \beta_{02}$ did not appreciably improve the fits. The β''_{0I} extracted from the data are listed in Table IV and are very similar to the DWBA deformations for these states. The best fits occurred for positive β''_{0I} except for the ^{84}Kr 0_2^+ state. The DWBA analysis of course does not determine the sign of β_I .

Figure 6 shows the resulting fits (solid curves) for the ^{84}Kr 0_2^+ and 2_2^- states. The 0_2^+ cross section is fitted best at forward angles with coupled channels and is fitted best at backward angles with the DWBA. In any case, the state definitely is $I^\pi = 0^+$ and has a monopole deformation between -0.10 and -0.20 . On the other hand, the calculated angular distribution to the 2_2^- state does not depend strongly on the path through the 2_1^+ state and gives a somewhat reasonable fit to the data with a one-phonon deformation parameter nearly one-half of the 2_1^+ state. The calculated cross sections to the two ^{84}Kr 4^+ states are shown in Fig. 7. Neither

DWBA nor coupled channels can reproduce the rather flat shape of the 4_1^+ angular distribution, whereas coupled channels provide an excellent fit to the 4_2^+ cross section.

The results for the two possible two-quadrupole phonon states in ^{86}Kr are shown in Fig. 8. The fit to the 4_1^+ cross section is very good, particularly at forward angles. Both the DWBA and coupled channels under estimate the very pronounced 80° maximum in the 2_2^+ angular distribution by a factor of 2.

3. Octupole-quadrupole phonon states

Finally, cross sections were calculated for $1^-, 2^-, 3^-, 4^-,$ and 5^- octupole-quadrupole states in ^{84}Kr . The angular distributions of the one-quadrupole phonon state at 0.882 MeV and the one-octupole phonon state at 2.705 MeV are fitted well with $\beta_2=0.128$ and $\beta_3=0.155$ and fixing these deformations, cross sections were calculated for the expected octupole-quadrupole states near 3.59 MeV which is the sum of the 2_1^+ and 3_1^- energies. The 2^- and 4^- strengths are predicted to be very small; however, those for the $1^-, 3^-,$ and 5^- states are not and are compared with possible experimental candidates for these states in Fig. 9. The coupled-channel results (dashed curves) have been multiplied by the factors shown in parentheses in order to have the same strength as the experimental cross sections. Although the excitation energies of this triplet of states are correct for them to be octupole-quadrupole vibrations, the calculated cross sections have the wrong shape and are too small in magnitude. There are many states in this excitation energy region and probably nearby states with the same spins and parities are heavily mixed with the predicted¹ octupole-quadrupole phonon states. This mixing would surely affect the cross sections to these states.

V. DISCUSSION AND CONCLUSIONS

Differential cross sections have been measured for 12.0-MeV elastic and inelastic proton scattering from thirteen states in ^{84}Kr and nine states in ^{86}Kr . Optical-model parameters have been extracted from the elastic cross sections and used in DWBA and coupled-channel analyses of the inelastic data. Tables I and II list the energies and I^π assignments of ^{84}Kr and ^{86}Kr levels, respectively, as determined from the present experiment and recent reports from other workers. The present excitation energies for ^{84}Kr levels

agree fairly well with those from Hill and Wang.⁵ For ^{86}Kr levels the agreement is best with Tucker *et al.*¹² In addition to the states already identified by previous workers we observe many new states at higher excitation in these nuclei.

Spin and parity assignments of $0^+, 4^+,$ and 4^+ to the "two-phonon" levels at 1.834, 2.086, and 2.337 MeV of excitation, respectively, and 3^- to the one-octupole phonon state at 2.705 MeV excitation in ^{84}Kr confirm the previous assignments for these levels, whereas our rather firm 2^+ assignment to 2.775-MeV level contradicts the possible 5^- assignment made by Hattula *et al.*⁷ The spins and parities of the remaining states in ^{84}Kr agree with the assignments made by Hill and Wang.⁵ The determination of ^{86}Kr spins and parities for the one- and "two-phonon" states agree well with those made by other workers^{10, 12, 13}; however, the present 4^+ fits to the 4.175- and 4.928-MeV levels contradict the 2^+ assignments from the (t, p) measurements.¹³ In addition, the 4^+ fit to the 3.330-MeV level does not agree with the conclusions of Tucker *et al.*¹² Most of the angular distributions to the higher excited states are either nearly isotropic or symmetric around 90° and can only be fitted with deformation parameters of around 0.05 to 0.10. Hence, important compound-nuclear contributions to the (p, p') cross sections of these states cannot be excluded, and perhaps the fits in some cases are fortuitous and should be considered speculative.

The cross sections to the one-phonon 2^+ and 3^- states are fitted well with the DWBA; the coupling to the elastic channel is small. In general the two-quadrupole phonon states are not very pure and much of their excitation proceeds through the direct transition to their one-phonon components. It is interesting to note that the magnitude and shape of the cross sections to the 2_2^+ states in ^{84}Kr and ^{86}Kr differ appreciably from each other and the theoretical calculations. Only one of the two low-lying 4^+ states in ^{84}Kr is described well as a two-phonon vibration and its angular distribution is almost identical to the corresponding state in ^{86}Kr . The ^{86}Kr 2.715-MeV 0^+ state contains an appreciable fraction of the pair-vibrational strength¹³; however, it could contain a large two-phonon amplitude. Its angular distribution could only be measured at very backward angles. The DWBA and coupled-channel deformation parameters for the one-phonon and two-phonon states are summarized in Tables IV and V. Considerably more experimental and theoretical work is required to understand fully the nature of the low-lying levels of these nuclei.

- †Research supported in part by U.S. Atomic Energy Commission.
- *Present address: Oak Ridge National Laboratory, Oak Ridge, Tennessee 37830.
- ‡Permanent address: Department of Physics, University of Notre Dame, Notre Dame, Indiana 46556.
- ¹A. Bohr, *K. Dan. Vidensk. Selsk. Mat.-Fys. Medd.* **26**, No. 14 (1952).
- ²T. Tamura, *Rev. Mod. Phys.* **37**, 679 (1965).
- ³T. Tamura, *Annu. Rev. Nucl. Sci.* **19**, 132 (1969).
- ⁴J. A. Deye, R. L. Robinson, and J. L. C. Ford, Jr., *Nucl. Phys.* **A180**, 449 (1972), and references contained therein.
- ⁵J. C. Hill and K. H. Wang, *Phys. Rev. C* **5**, 805 (1972).
- ⁶N. R. Johnson and G. D. O'Kelley, *Phys. Rev.* **108**, 82 (1957).
- ⁷T. Hattula, S. Andre, F. Schussler, and A. Moussa, *Nucl. Phys.* **A158**, 625 (1970).
- ⁸E. T. Williams and C. D. Coryell, *Phys. Rev.* **144**, 945 (1966).
- ⁹A. Ludán, *Z. Phys.* **236**, 403 (1970).
- ¹⁰E. Achterberg, F. C. Iglesias, A. E. Jech, J. A. Movagues, M. L. Pérez, J. J. Rossi, W. Scheuer, and J. F. Suárez, *Phys. Rev. C* **5**, 1587 (1972).
- ¹¹B. Rosner and E. J. Schneid, *Nucl. Phys.* **82**, 182 (1966).
- ¹²A. B. Tucker, K. E. Apt, J. D. Knight, and C. J. Orth, *Phys. Rev. C* **6**, 2075 (1972).
- ¹³P. J. Riley, D. K. Olsen, E. R. Flynn, J. D. Sherman, and N. Stein, *Bull. Am. Phys. Soc.* **19**, 450 (1974).
- ¹⁴C. G. Mattsson, S. E. Arnell, and L. Johnson, *Phys. Scr.* **5**, 58 (1972).
- ¹⁵N. P. Heydenburg, G. F. Pieber, and C. E. Anderson, *Phys. Rev.* **108**, 106 (1957).
- ¹⁶D. G. McCauley and J. E. Draper, *Phys. Rev. C* **4**, 475 (1971).
- ¹⁷C. L. Hollas, H. R. Hiddleston, V. D. Mistry, S. Sen, and P. J. Riley, *Phys. Rev. C* **5**, 1646 (1972).
- ¹⁸E. A. Silverstein, *Nucl. Instrum. Methods* **4**, 53 (1959).
- ¹⁹C. Williamson and J. P. Boujot, Saclay Report No. CEA 2189, 1962 (unpublished).
- ²⁰W. R. Smith, private communication.
- ²¹F. G. Perey, *Phys. Rev.* **131**, 745 (1963).
- ²²T. Tamura, ORNL Report No. ORNL-4152, 1967 (unpublished).